Br. J. Pharmacol. (1994), **111**, 1355–1360

Activation of chloride current by P_2-purinoceptors in rat ventricular myocytes

[1]M. Kaneda, K. Fukui & K. Doi

Department of Physiology, Yamagata University School of Medicine, Yamagata 990-23, Japan

1 Rat ventricular myocytes were dissociated and their responses to extracellularly applied ATP were recorded using patch pipettes under the whole cell configuration.

2 ATP initially induced an inward current followed by an outward current at − 50 mV. With a Cs-rich pipette solution the late outward current was blocked, leaving a sustained inward current (I_{ATPs}) suggesting that a K^+ conductance underlies the late response.

3 When the extracellular Cl^- concentration was changed, the reversal potential of I_{ATPs} corresponded well to the shift of the Cl^- equilibrium potential. I_{ATPs} was reversibly blocked by the chloride channel blocker, 4,4′-diisothiocyanatostilbene-2,2′-disulphonic acid (DIDS).

4 The concentration-response curve of I_{ATPs} had a Hill coefficient of 0.98 and an EC_{50} value of 5.2×10^{-6} M.

5 ATP was more potent than ADP, while AMP and adenosine were ineffective, suggesting that P_2-purinoceptor activation induced I_{ATPs}.

6 The activation of I_{ATPs} was depressed by depleting the extracellular Mg^{2+} and increased by adding Mg^{2+}.

7 Our results strongly suggest that P_2-purinoceptor activation by ATP induces both a Cl^--conductance (I_{ATPs}) and a K^+-conductance in rat ventricular myocytes.

Keywords: Ventricular myocytes; ATP; chloride current; P_2-purinoceptor

Introduction

There are many reports that adenosine 5′-triphosphate (ATP) acts as a neurotransmitter through activation of P_2-purinoceptors in a variety of tissues (Hoyle & Burnstock, 1991). In the heart, after the establishment of the presence of P_{2x}-purinoceptors (frog: Hoyle & Burnstock, 1986; rat: Fleetwood & Gordon, 1987), later reports focused on the ionic mechanisms of purinoceptors in the heart. In guinea-pig atrium, it has been shown that ATP responses are mediated by an activation of Cl conductance (Matsuura & Ehara, 1992). However, the ionic mechanism in the rat ventricle is confusing. Christie *et al.* (1992) reported that the activation of P_2-purinoceptor phosphorylates extracellular membrane-bound proteins, leading to the activation of a channel which carries Na^+ and Ca^{2+}. On the other hand, Pùceat *et al.* (1991b) reported that ATP binding to a putative P_3-purinoceptor activates an electrically neutral HCO_3^--Cl^- exchanger causing intracellular acidification. The intracellular acidification was thought to induce an increase in $[Ca^{2+}]_i$ (Scamps & Vassort, 1990; Púceat *et al.*, 1991a) and finally the activation of a Ca-dependent cation conductance (Colquhoun *et al.*, 1981). Thus, the relationship between the ionic mechanisms of ATP-induced responses and the types of purinoceptors was unclear in the rat ventricle. In the present experiments, therefore, we have used the patch clamp recording method to analyse the ionic mechanisms of ATP-induced responses and the possible types of purinoceptors in rat ventricular myocytes. We find that activation of a P_2-purinoceptor induced two different conductances, a Cl^--dependent current and a K^+-dependent current, which have not been reported previously. In the discussion the possible relationship between Cl^- movement through an activation of P_2-purinoceptor and an ATP-induced intracellular acidification has been suggested.

[1] Author for correspondence at present address: Department of Pharmacology, University College London, Gower Street, London WC1E 6BT.

Methods

Preparation

Isolated myocytes were obtained from male Sprague-Dawley rats (300–400 g) by collagenase digestion (0.1 mg ml^{-1}, Yakult, Tokyo, Japan) (Powell & Twist, 1976). The isolated cells were collected by sedimentation. The pellet was diluted with control solution to give a final concentration of 10^5 cells ml^{-1}; 200 μl of cell suspension was transferred to concanavalin A (Sigma Chemical Co., St Louis, MO, USA)-coated dishes containing 5 ml of control solution (extracellular Ca^{2+} concentration ($[Ca^{2+}]_o$) = 0.1 mM). Within 1 h cells were anchored on the dish. Cells were kept at room temperature until use and $[Ca^{2+}]_o$ was gradually increased up to 1 mM just before use. Cells were viable for 6–8 h in the present experiments.

Solutions

External and internal solutions used in the present experiments are shown in Table 1. To isolate Cl^- conductance we used a N-methyl-D-glucamine (NMG)-rich solution intra- and extracellularly. In the NMG-rich solution replacement of the membrane-permeable cations (Na^+, K^+ and Ca^{2+}) by the membrane-impermeable cation, NMG, blocks cation conductances, background conductances (Hagiwara *et al.*, 1992), the Na-K pump and the Na-Ca exchanger (Kimura *et al.*, 1986; Mechmann & Pott, 1986). Second, the possibility of the passage of Mg^{2+} or contaminating Ca^{2+} through voltage-gated Ca channels was excluded with verapamil. Third, the movement of residual intracellular K^+ through voltage-gated K^+ channels was also inhibited by perfusing the cells intracellularly with tetraethyl ammonium (TEA). Fourth, the Na-K pump was directly inhibited by ouabain.

A rapid superfusion system was used for solution exchange (Suzuki *et al.*, 1990). In this system solution exchange around the cells was complete within 100 ms. All experiments were

Table 1 Composition of solutions

External solutions (in mM)

	NaCl	*NaH_2PO_4*	*KCl*	*$CaCl_2$*	*$MgCl_2$*	*HEPES*	*Glucose*	*NMG*
Control	144	0.33	5.4	1	2	5	10	
K-free	150	0.33		1	2	5	10	
NMG-rich					2	5	10	150

Solutions contained 0.1 mg ml^{-1} bovine serum albumin and 0.001% phenol red. pH was adjusted at 7.4 with NaOH (control and K-free) or HCl (NMG-rich). NMG-rich solutions contained 5 μM verapamil and 10 μM ouabain. NMG: N-methyl-D-glucamine.

Internal solutions (in mM)

	CsOH	*CsCl*	*EGTA*	*HEPES*	*AA*	*ATP*	*NaCr*	*$MgCl_2$*	*$CaCl_2$*	*NMG*	*TEACl*
Cs-rich	110	20	10	5	90	5	5	1	0.5		
NMG-rich			10	5		5		1		110	20

pH was adjusted at 7.2 with CsOH (Cs-rich) or HCl (NMG-rich). Final Cl^- concentration of NMG-rich solution was 101 mM. AA: aspartic acid. ATP salts used are as follows: Cs-rich, Na_2-ATP; NMG-rich, Tris ATP.

carried out at room temperature. Unless otherwise mentioned, experiments were repeated on at least 3 cells.

Current recording

Currents were recorded by use of a patch clamp recording system in the whole cell configuration (Hamill *et al.*, 1981). The resistance of fire polished patch pipettes, filled with internal solution was 5–10 MΩ. The outer wall of the pipette, except for the tip, was coated with apiezon wax dissolved in chloroform (Apiezon Products Ltd., London, U.K.) to reduce the capacitance. The reference electrode was an Ag-AgCl wire connected to the dish by a 140 mM NaCl agar bridge. Currents were recorded by a patch clamp amplifier (CEZ-2200, Nihon Kohden, Tokyo, Japan). The ramp pulse was generated by a function generator (FG-121B, NF Circuit Design Block Co. Ltd., Yokohama, Japan). Current and voltage signals were recorded on a video tape recorder (HV-S21, Mitsubishi, Tokyo, Japan) through a PCM processor (PCM-DP16, Shoshin EM Corp., Okazaki, Japan). Current and voltage signals were also monitored by a chartrecorder (WR3701, Graphtec, Yokohama, Japan). The recorded current and voltage signals were filtered at 1 kHz through a low pass filter (E3201-A, NF Circuit Design Block Co. Ltd., Yokohama, Japan) and analysed by an off-line computer (PC-9801RX, NEC, Tokyo, Japan). A hard copy of individual current-voltage (*I-V*) relationship was plotted by an X-Y plotter (MIPLOT III, Graphtec, Yokohama, Japan) through the off-line computer.

Correction of holding potential

In the present experiments the holding potential (V_H) was corrected for the effect of liquid junction potentials (Hagiwara & Ohmori, 1982).

Correction of chloride concentration

The equilibrium potential of Cl^- was calculated using the activity coefficient of Cl^-. The activity coefficient of Cl^- in NMG-Cl solution was aproximated by that in KCl solution. The activity coefficient of $[Cl^-]_o$ was estimated as 0.74 at 153 mM, 0.82 at 51 mM and 0.88 at 15 mM. The activity coefficient of the intracellular Cl^- concentration ($[Cl^-]_i$) was estimated as 0.77 when cells were fully perfused by NMG-rich intracellular solution ($[Cl^-]_i$ = 101 mM). The corrected $[Cl^-]_o$ and $[Cl^-]_i$ was expressed as the product of the activity coefficient and Cl^- concentration.

Results

ATP-induced response

As shown in Figure 1, the application of 10^{-5} M ATP induced a biphasic current response at a V_H of − 49 mV. The initial inward current was observed immediately after the start of ATP superfusion and was followed by a gradual outward current. Removal of ATP induced a further transient outward current. In the experiment shown in Figure 1, a Cs-rich pipette solution was used to suppress outward K^+ conductances. The gradual loss of the ATP-induced outward current (compare 3 min and 42 min) probably reflects equilibration of this Cs-containing pipette solution with the intracellular medium. Moreover, as the outward current was not observed when cells were held at − 89 mV (not shown), this current may be carried by K^+. Separation of the inward and outward responses was performed by subtraction of the response recorded at 97 min from that at 3 min (Figure 1, subtract). The outward response reached a peak at around 10 s and decayed gradually. The average time after patch rupture until the disappearance of the outward current was 21.5 ± 7.5 min (n = 23). Out of 57 cells tested at 4 min after the establishment of intracellular perfusion, 52 had both an inward and an outward current and 5 cells had only an inward current. In the present experiment we have analysed only the sustained inward current (I_{ATPs}) in detail.

I_{ATPs} was repeatedly evoked when 10^{-4} M ATP was applied every 4 min. Therefore, in the present experiments the interval of ATP application was set at 4–5 min.

Ionic selectivity of I_{ATPs}

In previous reports, two different cation conductances activated by ATP have been reported in rat ventricular myocytes; a cation conductance (Christie *et al.*, 1992), and a Ca-dependent cation conductance (Púceat *et al.*, 1991a). In our experiments, cells were intra- and extracellularly perfused with an NMG-rich solution designed to block cation conductances (see Methods). However, even under these ionic conditions, the application of ATP induced I_{ATPs}. In the NMG-rich solution the average time until the isolation of I_{ATPs} was 7.7 ± 2.9 min (n = 42). Therefore, we conclude that I_{ATPs} response is not mediated by an increase in cation conductance. In addition, I_{ATPs} could be observed when an NMG-rich solution containing 10 mM EGTA was used for the extracellular perfusate, suggesting that an influx of Ca^{2+} is not involved in the generation of I_{ATPs}.

The Cl^--sensitive nature of I_{ATPs} was indicated by measurement of the reversal potential. In the experiment shown in Figure 2a, ATP was applied at various holding potentials. The response was sustained during the application of ATP at every membrane potential and reversed between − 5 and − 15 mV. The peak amplitude voltage relation plotted in Figure 2b, was linear and indicated a reversal potential (E_{ATPs}) of − 12 mV. In 6 experiments E_{ATPs} was − 13.3 ± 1.7 mV. This value is quite close to the equilibrium potential for Cl^- (E_{Cl}) of − 9.5 mV.

To facilitate the measurement of E_{ATPs}, the *I-V* relation was determined by the use of a ramp pulse (Figure 3a). The background conductance obtained before the application of ATP showed an outward going rectification. When $[Cl^-]_o$ and $[Cl^-]_i$ were 153 and 101 mM, respectively, the *I-V* curve in the presence of ATP showed large slope conductance and crossed with the control *I-V* curve at 0 mV (Figure 3b, left). When $[Cl^-]_o$ was reduced to 15 mM, the *I-V* curve also showed rectification and two *I-V* curves determined before and after ATP application crossed at + 31 mV (Figure 3b, right). The difference obtained by subtracting the control *I-V* curve from those in the presence of ATP was almost linear in every case (Figure 3c). The reversal potentials thus determined were corrected for the liquid junction potential and plotted against the activity of $[Cl^-]_o$ (Figure 4). These values corresponded well with the shift of Cl^- equilibrium potential calculated from the Nernst equation. When $[Cl^-]_o$ was changed from 153 mM to 15 mM, for a theoretical shift of Cl^- equilibrium potential of 54.1 mV, the observed shift of E_{ATPs} was 38.2 mV.

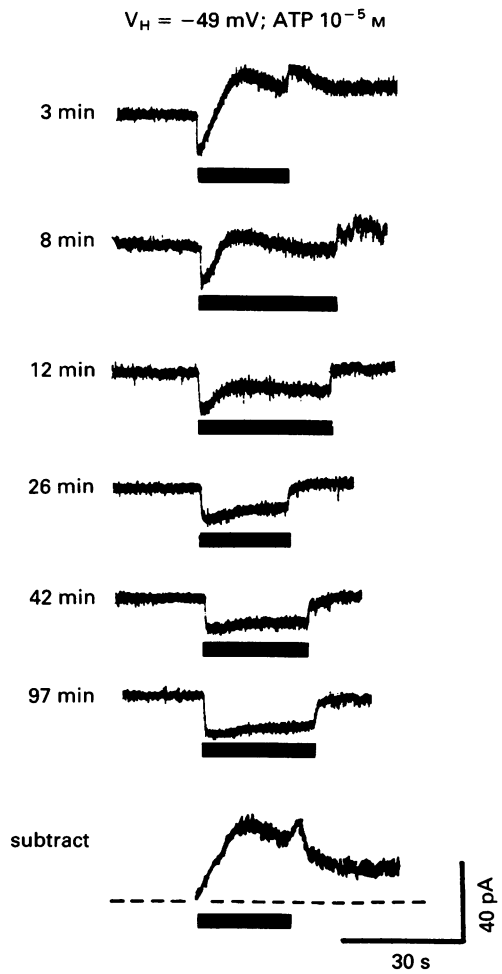

Figure 1 ATP-induced current recorded at different times. Times shown at the left, indicate the time after the establishment of the intracellular perfusion. Bars shown below each trace correspond to the duration of ATP application. V_H = − 49 mV. External solution: K-free, pipette solution: Cs-rich.

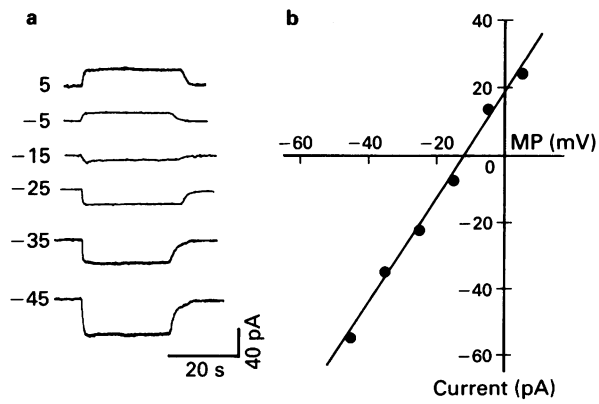

Figure 2 Current-voltage (*I-V*) relationship of I_{ATPs}. (a) I_{ATPs}s recorded at different holding potentials. (b) *I-V* relationship of I_{ATPs}. (a) and (b) were obtained from the same cell. Applied ATP concentration: 10^{-5} M, external solution: NMG-rich, pipette solution: NMG-rich.

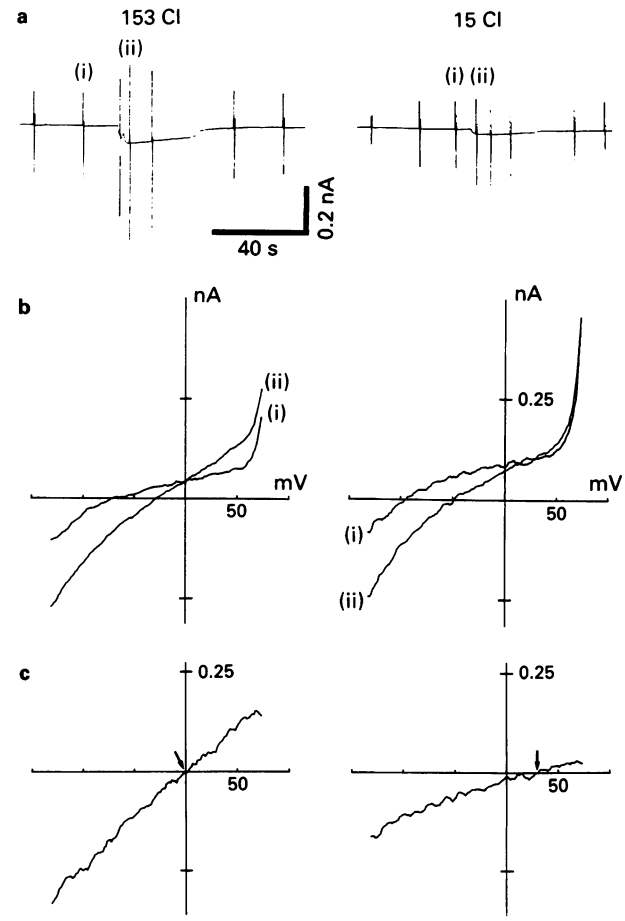

Figure 3 *I-V* relationship of I_{ATPs}. (a) Reponse to ramp pulse application. The sharp vertical lines on the current trace indicate the current evoked by the ramp pulse. Speed of ramp pulse was 420 mV s^{-1} (range − 140 mV to 70 mV). In the presence of ATP, ramp pulse was applied at around the peak of I_{ATPs}. (b) Estimation of E_{ATPs} by the ramp pulse. Individual *I-V* relationships correspond to (i) and (ii) shown in (a). The crossing points correspond to E_{ATPs}. (c) Subtraction of ramp pulse in the presence and absence of ATP. Arrows indicate E_{ATPs}. Applied ATP concentration: 10^{-5} M, external solution: NMG-rich, pipette solution: NMG-rich.

Effects of DIDS on I_{ATPs}

The Cl^--sensitive nature of I_{ATPs} was further confirmed by the use of Cl^- channel blocker, DIDS (de Lisle & Hopfer, 1986). In the presence of 0.2 mM DIDS, I_{ATPs} induced by 10^{-5} M ATP was suppressed by 70% (Figure 5). The inhibitory effects of DIDS on I_{ATPs} was reversible. The average of inhibition was 61 ± 8% ($n = 3$).

Response to various purinoceptor agonists

Purinoceptors can be pharmacologically classified into P_1 and P_2 types; P_1 was characterized by a high affinity for AMP and adenosine while P_2 is characterized by the high affinity for ATP and ADP (Burnstock, 1978). At a V_H of −45 mV, 10^{-5} M ATP induced I_{ATPs} (Figure 6). Similarly 10^{-4} M ADP also evoked I_{ATPs}, though the amplitude of I_{ATPs} was only 15% of that evoked by 10^{-5} M ATP. In contrast, AMP and adenosine did not evoke any response at 10^{-4} M (Figure 6). These results indicate that I_{ATPs} is mediated by a P_2-purinoceptor in the rat ventricular myocytes.

However, the P_{2X}-purinoceptor agonist, α, β-methyl-adenosine 5′-phosphate (AMP-CPP) and β, γ-methyl-adenosine 5′-phosphate (AMP-PCP) (Burnstock, 1990; Olsson & Pearson, 1990) did not evoke any response at 10^{-4} M (not shown). The subtype classification of P_2-purinoceptor therefore remains to be determined although our data might also indicate the presence of P_{2Y}-purinoceptors in rat ventricular myocytes (Björnsson *et al.*, 1989).

Concentration-response relationship of I_{ATPs}

At a V_H of −45 mV, application of 3×10^{-7} M ATP failed to evoke a detectable response (Figure 7a). I_{ATPs} was first observed at 6×10^{-7} M ATP and I_{ATPs} increased its amplitude with increasing ATP concentration. Figure 7b shows the concentration-response relationship of I_{ATPs}. In this figure the amplitude of individual responses was normalized to the amplitude of I_{ATPs} evoked by 10^{-5} M ATP. I_{ATPs} had a threshold at around 3×10^{-7} M and increased its amplitude in a sigmoidal fashion with increasing ATP concentration. The half maximal response was obtained at 5.2×10^{-6} M. At 10^{-4} M I_{ATPs} reached maximum. The concentration-response relationship of I_{ATPs} was fitted by the following equation:

$$I = I_{max}(C^n/(C^n + EC_{50}{}^n))$$

where I is the observed I_{ATPs}, I_{max} is the maximum current, C is the applied ATP concentration, EC_{50} is the ATP concen-

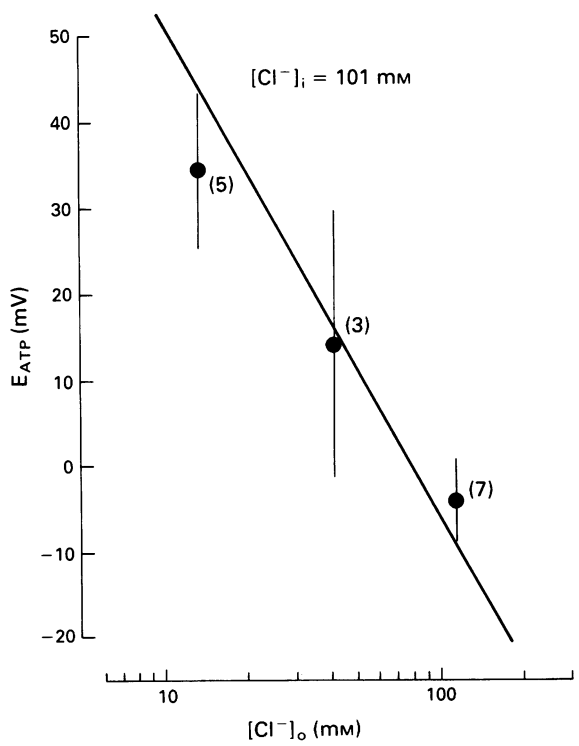

Figure 4 Relationship between $[Cl^-]_o$ and E_{ATPs}. $[Cl^-]_o$ was corrected by the activity coefficient of Cl^-. E_{ATPs} were corrected by the tip potential and the liquid junction potential. Symbols show the average with s.d. Solid line represents the equilibrium potential of Cl^- calculated from the Nernst equation. Number in parentheses indicates n values. Applied ATP concentration: 10^{-5} M, external solution: NMG-rich, pipette solution: NMG-rich.

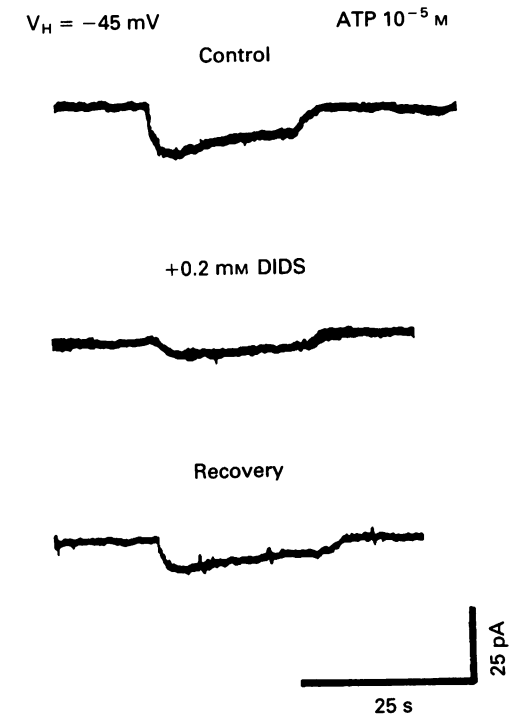

Figure 5 Effects of DIDS on I_{ATPs}. DIDS was perfused for 30 s prior to the ATP application. $V_H = -45$ mV. Applied ATP concentration: 10^{-5} M, external solution: NMG-rich, pipette solution: NMG-rich.

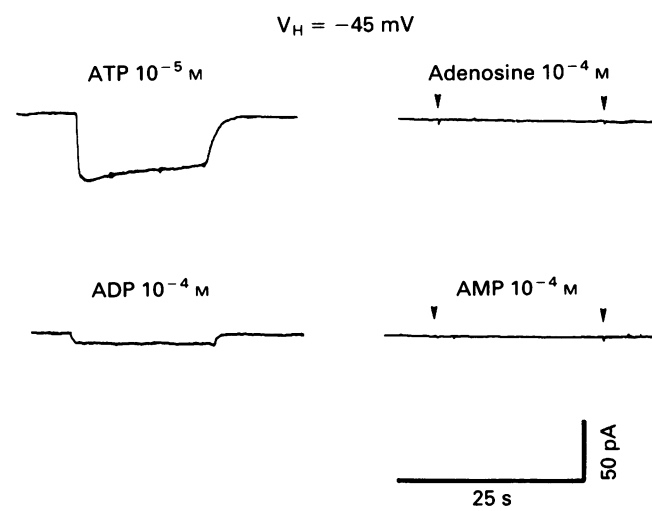

Figure 6 Responses to purinoceptor agonists. Arrows shown in the trace of AMP and adenosine indicate the start and the finish of the application. All responses are recorded from the same cell. $V_H = -45$ mV. External solution: NMG-rich, pipette solution: NMG-rich.

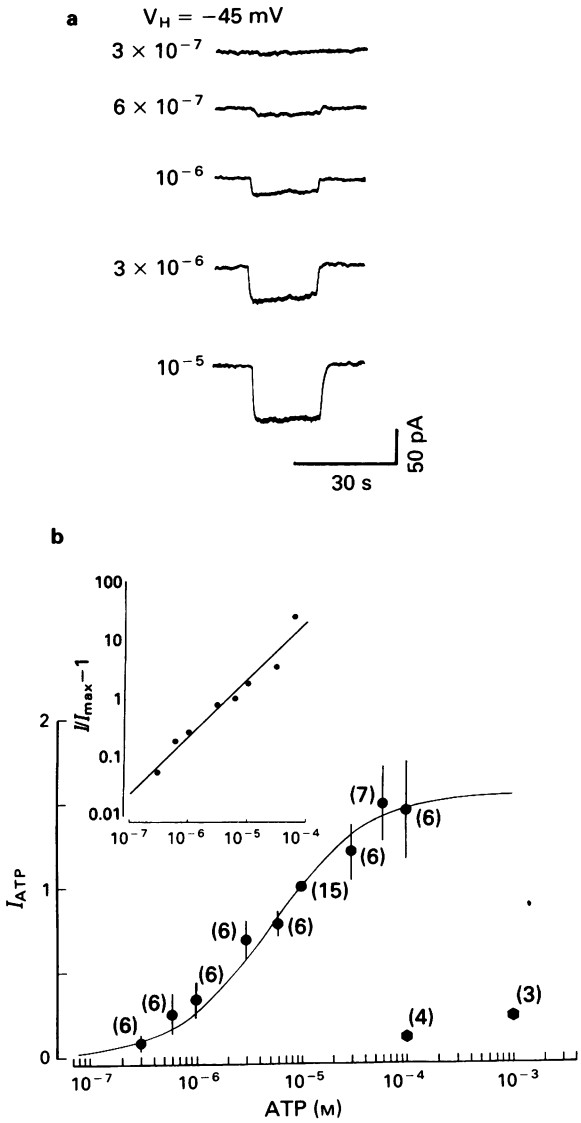

Figure 7 (a) I_{ATPs} evoked by different ATP concentrations (M) B. (b) Concentration-response relationship of I_{ATPs}. I_{ATPs} were normalized by I_{ATPs} evoked by 10^{-5} M ATP and plotted against ATP concentration. Symbols shown in the figure indicate the average with s.d. Numbers in parentheses indicate n values. Inset shows the Hill plot of I_{ATPs}. Solid line was drawn by the least squares method. V_H = − 45 mV. External solution: NMG-rich, pipette solution: NMG-rich. (●): ATP; (◆): ADP.

tration that evokes half maximal response, and n is the Hill coefficient. From the Hill plot of peak I_{ATPs} (inset), the Hill coefficient was determined as 0.98, indicating that the binding of one ATP molecule to P_2-purinoceptors activates I_{ATPs} in rat ventricular myocytes. Individual EC_{50} was also determined by the same equation in 7 cells having more than 5 points. An average of EC_{50} was $7.15 \times 10^{-6} \pm 6.20 \times 10^{-6}$ M (mean ± s.d.). In the Cs-rich solution the concentration-response relationship of I_{ATPs} was fitted by the similar parameters (EC_{50}, 2.2×10^{-6} M; Hill coefficient, 0.95).

Effects of extracellular Mg^{2+} ($[Mg^{2+}]_o$) on I_{ATPs}

It has been reported that ATP responses are sensitive to $[Mg^{2+}]_o$ (Scamps *et al.*, 1990). We tested the effect of $[Mg^{2+}]_o$ on I_{ATPs} evoked by 10^{-5} M ATP (Cs-rich pipette solution; Figure 8). The individual currents evoked at different $[Mg^{2+}]_o$ were normalized to the I_{ATPs} evoked in 2 mM Mg^{2+}. Then, normalized currents were averaged and plotted against

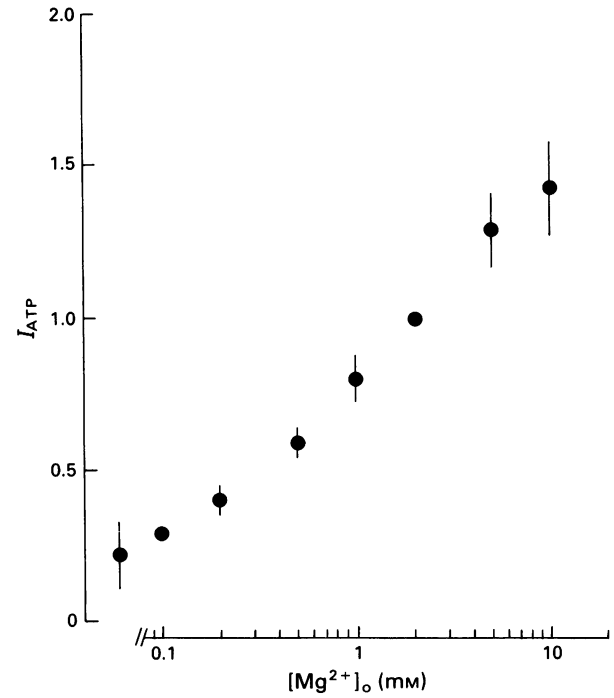

Figure 8 Effects of $[Mg^{2+}]_o$ on I_{ATPs}. I_{ATPs} were normalized by I_{ATPs} evoked in 2 mM $[Mg^{2+}]_o$. Concentration of applied ATP was 10^{-5} M. $MgCl_2$ was used for $[Mg^{2+}]_o$ change. Symbols show the average with s.d. V_H = − 49 mV. External solution: K-free, pipette solution: Cs-rich.

$[Mg^{2+}]_o$. When cells were perfused with Mg^{2+}-free solution, the observed amplitude of I_{ATPs} was 22 ± 11% of that obtained in 2 mM Mg^{2+} (n = 5). I_{ATPs} increased its amplitude with increasing $[Mg^{2+}]_o$. In 10 mM Mg^{2+} the amplitude of I_{ATPs} was 1.4 times larger than in 2 mM Mg^{2+} (n = 7). Thus in rat ventricular myocytes I_{ATPs} is affected by $[Mg^{2+}]_o$.

Discussion

We have identified an ATP-activated Cl^--current in rat ventricular myocytes by the intra- and extracellular perfusion of Na, K, Ca-free NMG solution. Under these conditions, the only permeant ions are anions, including Cl^-. In fact, the shift of E_{ATPs} fitted well to the theoretical value of E_{Cl} calculated from the Nernst equation, strongly suggesting that I_{ATPs} is carried by Cl^-. A similar ATP-induced Cl^- current was recently identified in guinea-pig atrial cells (Matsuura & Ehara, 1992).

In the present experiments we also observed ATP-induced K^+ currents. Thus, in ventricular myocytes, P_2-purinoceptors activation appears to induce both Cl^-- and K^+-conductances independently. In previous reports it has been shown that ATP activates two different types of conductances in guinea-pig (Hirano *et al.*, 1991) and bullfrog atria (Friel & Bean, 1988), one component of which was considered to be carried by K^+. In bullfrog atrium, ATP-induced K^+ conductances are thought to be identical to muscarinic ATP-induced K^+ conductances, which do not exist in ventricular cells (Friel & Bean, 1988). Thus, it would be interesting to see if ATP-induced K^+ conductances are sharing same K^+ channels with other K^+ conductances in rat ventricular myocytes.

In symmetrical Cl^- I_{ATPs} reversed its polarity at around 0 mV and had a linear I-V relationship. Previous studies of ATP-currents reported linear I-V relationships and reversal potentials around 0 mV in symmetrical Cl^- solution in the rat ventricular myocytes (Scamps & Vassort, 1990; Christie *et al.*, 1992). From the characteristics of I-V curve these authors

considered the existence of cation conductances. In the present experiments, however, the observed I_{ATPs} was mediated by Cl^-. Therefore, we conclude that the ATP-induced conductance having a linear *I-V* relationship is mediated by Cl^- and not by cations.

In the rat ventricular myocytes, previous reports show an increase in $[Ca^{2+}]_i$ by an application of ATP (Danziger *et al.*, 1988; Björnsson *et al.*, 1989; de Young & Scarpa, 1987, 1989). In ventricular myocytes, the equilibrium potential for Cl^- is thought to be more positive than the resting potential. Activation of I_{ATPs} would therefore induce depolarization within a few seconds. In fact, ATP-induced depolarization has been reported in rat ventricular myocytes, where superimposition of action potentials occurs within 1–2 s after the start of depolarization (Christie *et al.*, 1992). Therefore, $[Ca^{2+}]_i$ increase as a result of the activation of voltage-gated Ca^{2+} channels was considered. Actually this hypothesis corresponds well to the previous observation of simultaneous recording of membrane potentials and $[Ca^{2+}]_i$ in the rat (Björnsson *et al.*, 1989). As to the initiation of an increase in $[Ca^{2+}]_i$ the possibilities of the involvement of the intracellular acidification by a putative P_3-purinoceptor (Púceat *et al.*, 1991b) and extracellular membrane phosphorylation (Christie *et al.*, 1992) have been reported. However, these two possibilities are not likely to be the triggering mechanism since it seems difficult to explain the time course of $[Ca^{2+}]_i$ increase by these mechanisms. Using fluorescent dyes they reported that the increase in $[Ca^{2+}]_i$ reached a peak at around 15–20 s after the ATP application and then elevated $[Ca^{2+}]_i$ started to return to the control level. On the other hand, peak responses for both intracellular acidification (Púceat *et al.*, 1991b) and extracellular phosphorylation (Christie *et al.*, 1992) were observed at 60 s after the ATP application. Thus, $[Ca^{2+}]_i$ increase reached a peak before the other two responses reached that peak. Therefore, we concluded that the initiation of $[Ca^{2+}]_i$ increase was triggered by an activation of ATP-induced depolarization which is followed by voltage gated Ca^{2+} channel activation.

In the rat, it has been reported that ATP induces intracellular acidification by the activation of a putative P_3-purinoceptor which is coupled to a HCO_3^--Cl^- exchanger (Púceat *et al.*, 1991b). In the present experiments we found P_2-purinoceptor-activated Cl^- conductance. If the activation of I_{ATPs} occurs at the resting potential, Cl^- ions would move from the intracellular space to the extracellular space. This depletion of the intracellular Cl^- could activate the HCO_3^--Cl^- exchanger leading to intracellular acidification. Thus, it is also possible to explain the previously reported intracellular acidification by the activation of a P_2-purinoceptor. Actually, the extracellular ATP concentrations which gave the threshold, EC_{50} and the maximal response of I_{ATPs} in the present experiments were similar to those reported for the ATP-induced intracellular acidification (Púceat *et al.*, 1991b). Thus, it will be interesting to see if the present result could explain some of the previous observation that have been ascribed to the existence of a putative P_3-purinoceptors.

We thank Professor G. Burnstock, Dr J. Kimura, Dr A. Noma and Dr M. Farrant for their critical comments and valuable discussion.

References

BJÖRNSSON, O.G., MONCK, J.R. & WILLIAMSON, J.R. (1989). Identification of P_{2Y}-purinoceptors associated with voltage-activated cation channels in cardiac ventricular myocytes of the rat. *Eur. J. Biochem*, **186**, 395–404.

BURNSTOCK, G. (1978). A basis for distinguishing two types of purinergic receptor. In *Cell Membrane Receptors for Drugs and Hormones: A Multidisciplinary Approach*, ed. Bolis, L. & Straub, R.B., pp. 107–118, New York: Raven Press.

BURNSTOCK, G. (1990). Overview-Purinergic mechanisms. In *Biological Actions of Extracellular ATP*. Ann. N.Y. Acad. Sci. ed. G.R. Dubyak & J.A. Fedan, Vol. 603, pp. 1–18, New York: New York Academy of Sciences.

CHRISTIE, A., SHARMA, V.K. & SHEU, S.-S. (1992). Mechanism of extracellular ATP-induced increase of cytosolic Ca^{2+} concentration in isolated rat ventricular myocytes. *J. Physiol.*, **445**, 369–388.

COLQUHOUN, D., NEHER, E., REUTER, H. & STEVENS, C.F. (1981). Inward current channels activated by intracellular Ca in cultured cardiac cells. *Nature*, **294**, 752–754.

DANZIGER, R.S., RAFFAELI, S., MORENO-SANCHEZ, R., SAKAI, M., CAPOGROSSI, M.C., SPURGEON, H.A., HANSFORD, R.G. & LAKATTA, E.G. (1988). Extracellular ATP has a potent effect to enhance cystolic calcium and contractility in single ventricular myocytes. *Cell Calcium*, **9**, 193–199.

FLEETWOOD, G. & GORDON, J.L. (1987). Purinoceptors in the rat heart. *Br. J. Pharmacol.*, **90**, 219–227.

FRIEL, D.D. & BEAN, B.P. (1988). Two ATP-activated conductances in bullfrog atrial cells. *J. Gen. Physiol.*, **91**, 1–27.

HAGIWARA, N., IRISAWA, H., KASANUKI, H. & HOSODA, S. (1992). Background current in sino-atrial node of the rabbit heart. *J. Physiol.*, **448**, 53–72.

HAGIWARA, S. & OHMORI, H. (1982). Studies of calcium channels in rat clonal pituitary cells with patch electrode voltage clamp. *J. Physiol.*, **331**, 231–252.

HAMILL, O.P., MARTY, A., NEHER, E., SAKMANN, B. & SIGWORTH, F.J. (1981). Improved patch-clamp techniques for high-resolution current recording from cells and cell-free membrane patches. *Pflügers Arch.*, **391**, 85–100.

HIRANO, Y., ABE, S., SAWANOBORI, T. & HIRAOKA, M. (1991). External ATP-induced changes in $[Ca^{2+}]_i$ and membrane currents in mammalian atrial myocytes. *Am. J. Physiol.*, **260**, C673–C680.

HOYLE, C.H.V. & BURNSTOCK, G. (1986). Evidence that ATP is a neurotransmitter in the frog heart. *Eur. J. Pharmacol.*, **124**, 285–289.

HOYLE, C.H.V. & BURNSTOCK, G. (1991). ATP receptors and their physiological roles. In *Adenosine in the Nervous-System*. ed. Stone, T.W. pp. 43–76, London: Academic Press.

KIMURA, J., NOMA, A. & IRISAWA, H. (1986). Na-Ca exchange in mammalian heart cells. *Nature*, **319**, 596–597.

DE LISLE, R.C. & HOPFER, U. (1986). Electrolyte permeabilities of pancreatic zymogen granules: implications for pancreatic secretion. *Am. J. Physiol.*, **250**, G489–G496.

MATSUURA, H. & EHARA, T. (1992). Activation of chloride current by purinergic stimulation in guinea pig heart cells. *Circ. Res.*, **70**, 851–855.

MECHMANN, S. & POTT, L. (1986). Identification of Na-Ca exchange current in single cardiac myocytes. *Nature*, **319**, 597–599.

OLSSON, R.A. & PEARSON, J.D. (1990). Cardiovascular purinoceptors. *Physiol. Rev.*, **70**, 761–845.

POWELL, T. & TWIST, V.W. (1976). A rapid technique for the isolation and purification of adult cardiac muscle cells having respiratory control and a tolerance to calcium. *Biochem. Biophys. Res. Commun.*, **72**, 327–333.

PÚCEAT, M., CLÉMENT, O., SCAMPS, F. & VASSORT, G. (1991a). Extracellular ATP-induced acidification leads to cytosolic calcium transient rise in single rat cardiac myocytes. *Biochem. J.*, **274**, 55–62.

PÚCEAT, M., CLÉMENT, O. & VASSORT, G. (1991b). Extracellular MgATP activates the Cl^-/HCO_3^- exchanger in single rat cardiac cells. *J. Physiol.*, **444**, 241–256.

SCAMPS, F., LEGSSYER, E., MAYOUX, E. & VASSORT, G. (1990). The mechanism of positive intropy induced by adenosine triphosphate in rat heart. *Circ. Res.*, **7**, 1007–1016.

SCAMPS, F. & VASSORT, G. (1990). Mechanism of extracellular ATP-induced depolarization in rat isolated ventricular cardiomyocytes. *Pflügers Arch.*, **417**, 309–316.

SUZUKI, S., TACHIBANA, M. & KANEKO, A. (1990). Effects of glycine and GABA on isolated bipolar cells of the mouse retina. *J. Physiol.*, **421**, 645–662.

DE YOUNG, M.B. & SCARPA, A. (1987). Extracellular ATP induces Ca^{2+} transients in cardiac myocytes which are potentiated by norepinephrine. *FEBS Lett.*, **223**, 53–58.

DE YOUNG, M.B. & SCARPA, A. (1989). ATP receptor-induced Ca^{2+} transients in cardiac myocytes: sources of mobilized Ca^{2+}. *Am. J. Physiol.*, **257**, C750–C758.

(Received November 17, 1993
Revised December 20, 1993
Accepted January 4, 1994)